DE GRUYTER OPEN

Acta Geophysica
vol. 64, no. 6, Dec. 2016, pp. 2232-2243
DOI: 10.1515/acgeo-2016-0097

An Easy Method for Interpretation of Gravity Anomalies Due to Vertical Finite Lines

İbrahim KARA and Nihan HOSKAN

Department of Geophysical Engineering, Faculty of Engineering, Istanbul University, Avcılar, Turkey; e-mail: nihan@istanbul.edu.tr

Abstract

A new method is introduced to determine the top and bottom depth of a vertical line using gravity anomalies. For this, gravity at a distance *x* from the origin and horizontal derivative at that point are utilized. A numerical value is obtained dividing the gravity at point *x* by horizontal derivative. Then a new equation is obtained dividing the theoretical gravity equation by the derivative equation. In that equation, assigning various values to the depth and length of vertical line, several new numerical values are obtained. Among these values, a curve is obtained for the one that is closest to the first value from attending the depth and length values. The intersection point of these curves obtained by repeating this procedure several times for different points *x* yield the real depth and length values of the line. The method is tested on two synthetics and field examples. Successful results are obtained in both applications.

Key words: gravity anomaly, vertical finite line, depth and length curves.

1. INTRODUCTION

Interpretation of the potential-based data is usually faced with multi-solution. For example, gravity anomalies of sphere and vertical line cannot be distinguished by naked eye. In most cases, lines are accepted to be lateral in evaluations (Odegard and Berg 1965, Gay 1965, Abdelrahman 1990,

Ownership: Institute of Geophysics, Polish Academy of Sciences;

Abdelrahman *et al.* 1989). For the interpretation of the spherical sources, Mohan *et al.* (1986) used the Mellin transform, Shaw and Agarwall (1990) applied the Walsh transform, Abdelrahman and H.M. El-Araby (1993) utilized correlation factors, and Abdelrahman and T.M. El-Araby (1993) operated the least squares approach. Gupta (1983) used the least squares technique for interpretation of the vertical infinite line and also Kara and Kanli (2005) developed nomograms for the vertical finite line. To analyze the gravity anomalies due to simple geometrical structures, several methods have been developed (Essa 2007a, 2011, 2012, 2014). In a study similar to the method presented in this work, Essa (2007b) calculated shape factor and source depths of a sphere, and horizontal and vertical infinite lines. However, in his study, measurement values should be very accurate, otherwise the method becomes unsuccessful.

In this study, a new method has been developed for determination of depth and length of vertical finite line. Here, along a profile, gravity and horizontal derivative values are utilized. In order to show the validity of the method, it is tested on two numerical examples and then top and bottom depths of the source body are determined assessing the Louga gravity anomaly (USA).

2. FORMULATION OF THE PROBLEM AND SOLUTION

The gravitational acceleration produced by a vertical line extending to a finite depth to the bottom at an observation point, P, displayed in Fig. 1, is expressed with the following relation by Nettleton (1942):

$$g(x) = A\left[\frac{1}{\left(x^2+h^2\right)^{1/2}} - \frac{1}{\left[x^2+\left(h+L\right)^2\right]^{1/2}}\right], \qquad (1)$$

where A is the amplitude coefficient ($A = G\rho_l$, where G is gravity constant, ρ_l is the linear density of anomalous mass in the line), h is the depth of upper surface , L is the length of the body, and x is the distance from observation point to the origin.

The horizontal derivative of Eq. 1 is:

$$g_x(x) = A\left[\frac{-x}{\left(x^2+h^2\right)^{3/2}} - \frac{-x}{\left[x^2+\left(h+L\right)^2\right]^{3/2}}\right], \qquad (2a)$$

but the horizontal first gradient values in the field study are obtained as:

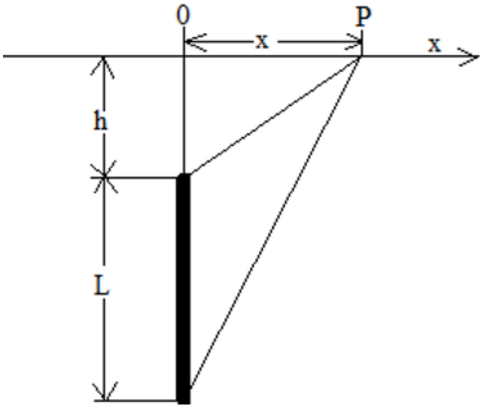

Fig. 1. Vertical line extending to a finite depth.

$$g_x(x) = \left[g\left(x + dx\right) - g\left(x - dx\right) \right] / 2dx \ , \tag{2b}$$

where dx is the grid-spacing.

If Eqs. 1 and 2 are divided by each other and left and right sides of the resulting equation are termed F_1 and F_2, respectively, the following equations are obtained:

$$F_1 = \frac{g(x)}{g_x(x)} \ , \tag{3a}$$

$$F_2 = \frac{\dfrac{1}{\left(x^2 + h^2\right)^{1/2}} - \dfrac{1}{\left[x^2 + \left(h + L\right)^2\right]^{1/2}}}{\dfrac{-x}{\left(x^2 + h^2\right)^{3/2}} - \dfrac{-x}{\left[x^2 + \left(h + L\right)^2\right]^{3/2}}} \ , \tag{3b}$$

where F_1 is obtained dividing the measurement value at any observation point ($x \neq 0$) by horizontal derivative value at the same point. Then, F_2 is computed for a small h value (for example $h = 1$) and increasing L values (for example $L = 1, 2, 3.....50$). Meanwhile, in each calculation, the difference between F_1 and F_2 is determined. For the least value of this difference, h and L values are saved. Then h is slightly increased (for example $h = 2$) and the same procedure is repeated. The values of h and L (as h is the vertical axis and L is the horizontal axis) obtained from here are plotted in a coordinate system and a curve is obtained. The flow chart of the method is illustrated in Fig. 2. This process is repeated several times for different observation points and the intersection point of curves drawn on the same co-

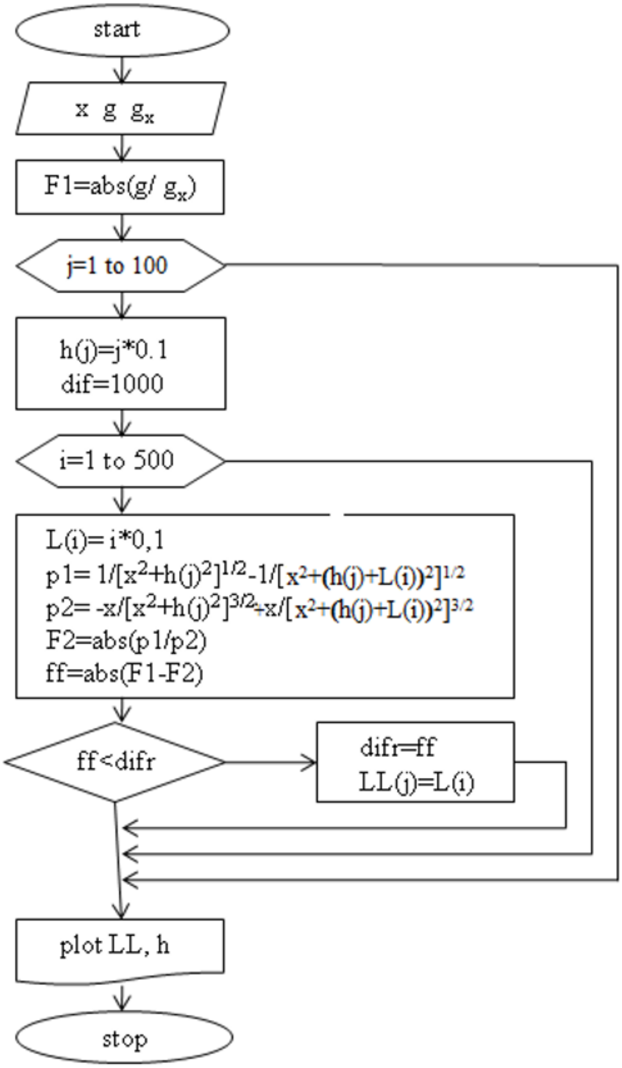

Fig. 2. The flow chart of the method for a single curve.

ordinate system yield the depth and length of the vertical line. If these curves do not intercept, it means that *h* or *L* or both are not sufficiently extended and they are extended until the intersection point of these curves is provided.

3. SYNTHETIC EXAMPLES

For testing the validity of the proposed method, the application is carried out on two theoretical models. In the first application, the gravity anomaly of a vertical finite line with $A = 100$ mGal*m, $h = 5$ m and $L = 30$ m is used (Fig. 3a).

The horizontal derivative anomaly of this anomaly is shown in Fig. 3b.

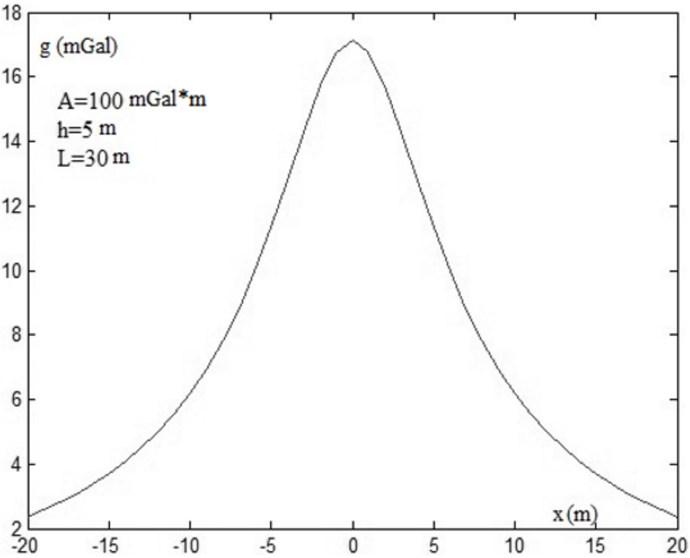

Fig. 3a. Gravity anomaly used in the first application.

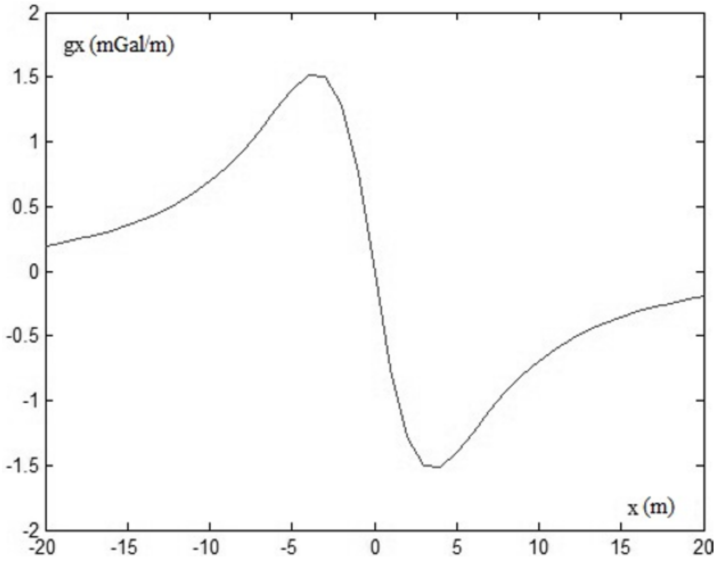

Fig. 3b. Horizontal derivative anomaly of the anomaly shown in Fig. 3a.

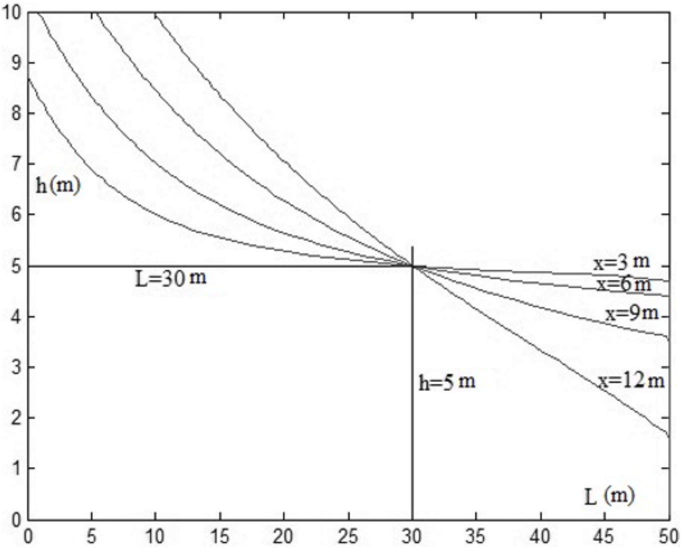

Fig. 3c. The curves obtained when the present method is applied to anomalies in Fig. 3a and b.

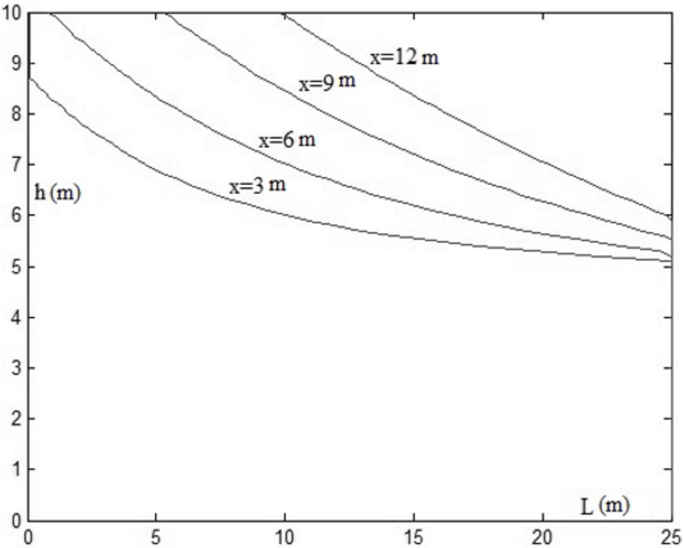

Fig. 3d. For the same application, the curves that are not intersecting due to insufficiently extended *L*.

Then the method is applied using gravity and horizontal derivative values at observation points $x = 3\text{-}6\text{-}9\text{-}12$ m and curves community given in Fig. 3c is obtained. As shown therein, $h = 5$ m and $L = 30$ m are found.

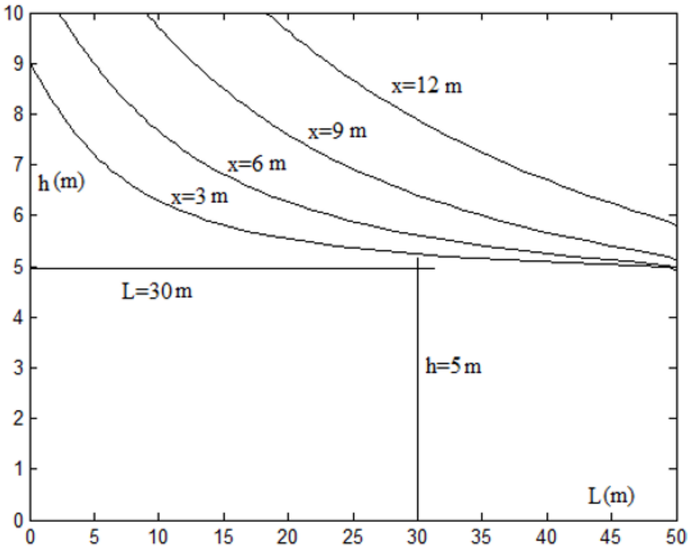

Fig. 3e. The curves obtained by adding 1 m to the reference level and applying the present method to the anomaly displayed in Fig. 3a.

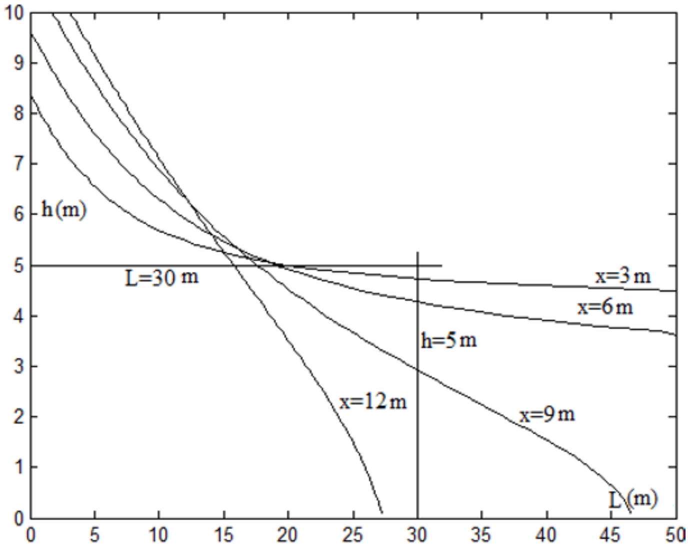

Fig. 3f. The curves obtained by subtracting 1 m from the reference level and applying the present method to the anomaly displayed in Fig. 3a.

These values are in excellent agreement with the initial parameters and this result indicates the validity of the present method. In addition, as mentioned previously, if h and L are chosen smaller than their real values, the curves have no tendency to cross each other. In this synthetic example, $L = 30$ m is taken. If Eq. 3b is calculated to $L = 25$ m and the curves are drawn, these curves do not cross each other (Fig. 3d).

In order for the curves to intersect each other, the value of L should be slightly increased, as illustrated in Fig. 3c. Besides, if the reference level of anomaly is detected incorrectly, the curves mentioned above either do not cross each other or intersect at the point that is far away from where they must intersect. Namely, intercepting the curves each other in one point depends on selecting the reference level correctly. For explaining the importance of this fact, Fig. 3e is obtained by adding 1 m and Fig. 3f is obtained by subtracting 1 m from the reference level of the anomaly displayed in Fig. 3a. Hence, using this method in practice, it must be changed several times with small intervals to the reference level of the anomaly until the intersection point of the curves with minimal dispersion is identified. Even though the curves still do not cross each other, the intersection point is accepted at the mid-point of the closest area of the curves.

For the second synthetic example, $A' = 1000$ mGal*m^2 and $h = 8$ m are chosen, using the following Eq. 4

$$g = A' \frac{h}{\left(x^2 + h^2\right)^{3/2}} , \tag{4}$$

from which the gravity anomaly of a sphere is obtained (here, $A' = 4/3\pi G R^3 \rho$). After horizontal derivative values of this sphere are calculated, using g and g_x values of this sphere at distances of $x = 3$-6-9-12 m, the

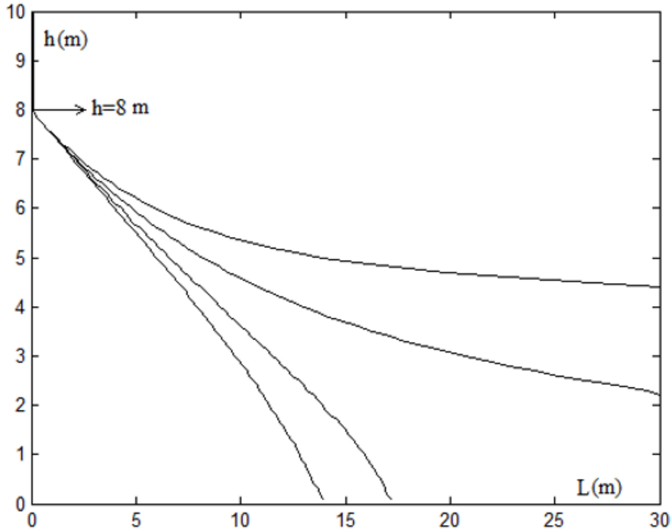

Fig. 4. Curve assemblage obtained for the second synthetic example (sphere).

proposed method is applied and the curves given in Fig. 4 are obtained. As shown in Fig. 4, the curves intersect at $h = 8$ m. In fact, the accepted h is at 8 m. However, careful inspection of Fig. 4 reveals that $L = 0$, indicating that the source body is a sphere.

4. FIELD EXAMPLE

For the field example, Louga gravity anomaly (USA) is used (Fig. 5a). The solid line in Fig. 5a represents observation values sampled in 1 km intervals. Thereafter, horizontal derivative values of the curve are obtained (Fig. 5b). The curves shown in Fig. 5c are obtained from application of the present method to gravity and horizontal derivative values at distance of $x = 2, 4, 6, 8$ km.

From the intersection point of curves, depth (h) and length (L) of the vertical finite line are found to be 5.75 and 16.3 km, respectively. Then in Eq. 1, x is taken as 0, and if h and L values calculated above and max gravity value in the anomaly is replaced in this equation, A is found as 602 mGal*Km. The values of A, h, and L computed above are replaced into Eq. 1 to find a new gravity anomaly (dotted line in Fig. 5a). It is seen that the observed and calculated anomalies are very close to each other.

In addition, Mohan *et al.* (1986) found the depth of sphere to be 9.31 km, applying the Mellin transform and assuming that Louga gravity anomaly belongs to a sphere. If this anomaly belongs to a sphere, the curves similar to those in Fig. 4 would be obtained. Thus, this anomaly is determined to be a vertical finite line.

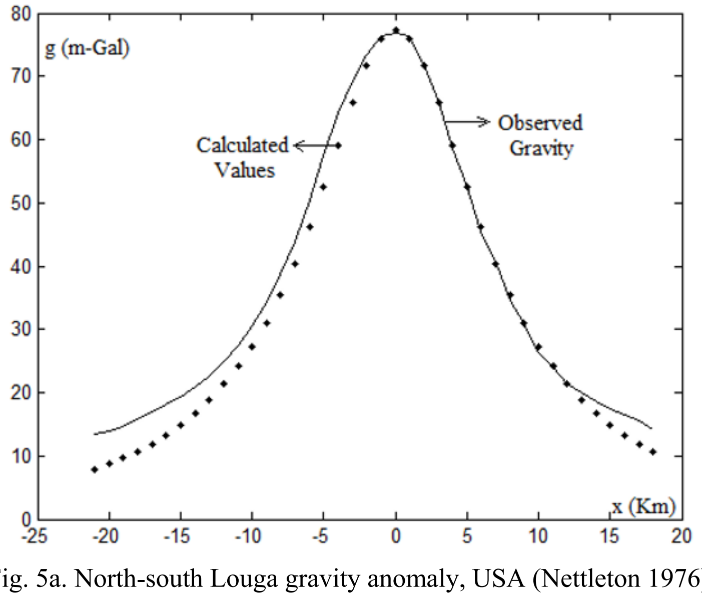

Fig. 5a. North-south Louga gravity anomaly, USA (Nettleton 1976).

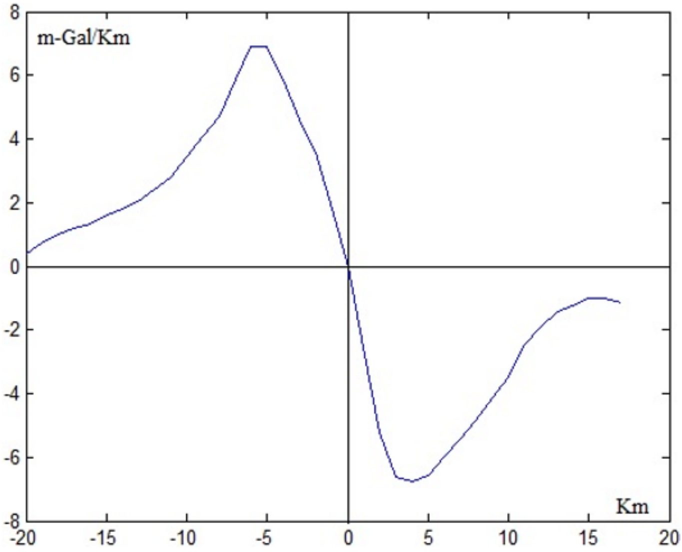

Fig. 5b. Horizontal first derivative anomaly of the Louga gravity anomaly.

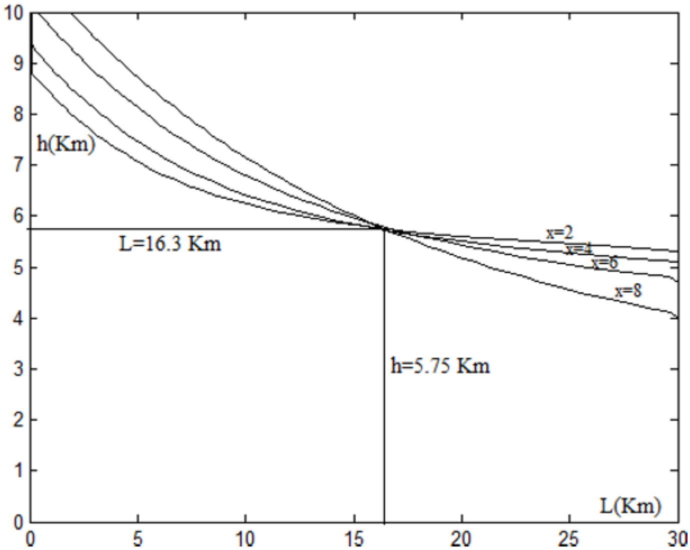

Fig. 5c. Curves obtained by the application of proposed method to the Louga gravity anomaly.

5. CONCLUSION

In this study, depth and length of a vertical finite line are determined by the interpretation of residual gravity anomaly of the source body. In this interpretation, the ratio of measurement values at any observation point to horizontal derivative values at the same point is obtained numerically and then, for various depths and lengths, the ratio of theoretical vertical finite line equation to theoretical horizontal derivative equality is computed. The calculated values are plotted length versus depth and a curve is obtained. This process is repeated for several observation points and several curves are plotted on the same coordinate axis. Intersection point of these curves reflects the real depth and length of vertical finite line.

In order for the method to be completed accurately, regional effects and the noises in the anomaly should be eliminated and the reference level should be determined accurately. Besides, if the anomaly has noises, since it is possible for a mistake to occur, particularly when calculating horizontal derivative values, the anomaly must be smoothed before applying the proposed method. Furthermore, if another body exists near the vertical line, the proposed method may become unsuccessful because the anomaly of this body affects the anomaly of the vertical line.

This method has been tested on two synthetic examples and applied to field anomaly and the results are compared with those of another author who previously assessed this anomaly.

Acknowledgements. We thank Editor and the anonymous reviewers for their detailed and constructive comments which helped to improve this article.

References

Abdelrahman, E.M. (1990), Magnetic interpretation of long horizontal cylinders using correlation factors between successive least-squares residual anomaly profiles, *Pure Appl. Geophys.* **132**, 3, 521-531, DOI: 10.1007/BF00876927.

Abdelrahman, E.M., and T.M. El-Araby (1993), A least-squares minimization approches to depth determination from moving average residual gravity anomalies, *Geophysics* **58**, 12, 1779-1784, DOI: 10.1190/1.1443392.

Abdelrahman, E.M., and H.M. El-Araby (1993), Shape and depth solutions from gravity data using correlation factors between succesive least-squares residual, *Geophysics* **58**, 12, 1785-1791, DOI: 10.1190/1.1443393.

Abdelrahman, E.M., A.I. Bayoumi, Y.E. Abdelhayt, M.M. Gobashy, and H.M. El-Araby (1989), Gravity interpretation using correlation factors between successive least-squares residual anomalies, *Geophysics* **54**, 12, 1614-1621, DOI: 10.1190/1.1442629.

Essa, K.S. (2007a), Gravity data interpretation using the s-curves method, *J. Geophys. Eng.* **4**, 2, 204-213, DOI: 10.1088/1742-2132/4/2/009.

Essa, K.S. (2007b), A simple formula for shape and depth determination from residual gravity anomalies, *Acta Geophys.* **55**, 2, 182-190, DOI: 10.2478/s11600-007-0003-9.

Essa, K.S. (2011), A new algorithm for gravity or self-potential data interpretation, *J. Geophys. Eng.* **8**, 3, 434-446, DOI: 10.1088/1742-2132/8/3/004.

Essa, K.S. (2012), A fast interpretation method for inverse modeling of residual gravity anomalies caused by simple geometry, *J. Geol. Res.* **2012**, 327037, DOI: 10.1155/2012/327037.

Essa, K.S. (2014), New fast least-squares algorithm for estimating the best-fitting parameters of some geometric-structures to measured gravity anomalies, *J. Adv. Res*. **5**,1, 57-65, DOI: 10.1016/j.jare.2012.11.006.

Gay, S.P. Jr. (1965), Standard curves for magnetic anomalies over long horizontal cylinders, *Geophysics* **30**, 5, 818-828, DOI: 10.1190/1.1439656.

Gupta, O.P. (1983), A least-squares approach to depth determination from gravity data, *Geophysics* **48**, 3, 357-360, DOI: 10.1190/1.1441473.

Kara, I., and A.I. Kanli (2005), Nomograms for interpretation of gravity anomalies of vertical cylinders, *J. Balkan Geophys. Soc.* **8**, 1, 1-6.

Mohan, N.L., L. Anandabadu, and R. Seshagari (1986), Gravity interpretation using the Melin transform, *Geophysics* **51**, 1, 114-122, DOI: 10.1190/1.1442024.

Nettleton, L.L. (1942), Gravity and magnetic calculation, *Geophysics* **7**, 3, 293-310, DOI: 10.1190/1.1445015.

Nettleton, L.L. (1976), *Gravity and Magnetic in Oil Prospecting*, McGraw-Hill Book Co.

Odegard, M.E., and J.W. Berg (1965), Gravity interpretation using the Fourier integral, *Geophysics* **30**, 3, 424-438, DOI: 10.1190/1.1439598.

Shaw, R.K., and B.N.P. Agarwall (1990), The application of Walsh transforms to interpret gravity anomalies due to some simple geometrically shaped causative sources: A feasibility study, *Geophysics* **55**, 7, 843-850, DOI: 10.1190/1.1442898.

Received 27 May 2015
Received in revised form 15 January 2016
Accepted 22 February 2016